

Supporting Information

Adie et al. 10.1073/pnas.1121193109

SI Text

Derivation of the Aberration Correction Filter. The dispersion-corrected spectral domain optical coherence tomography signal, $S(x, y, z; k)$, acquired through two-dimensional transverse scanning of the incident beam, can be written in terms of a two-dimensional convolution of the (complex) system point-spread function (PSF), $h(x, y, z; k)$, with the scattering potential $\eta(x, y, z)$ (1, 2)

$$S(x, y, z; k) = \iiint h(x - x', y - y', z'; k) \eta(x', y', z') dx' dy' dz'. \quad [\text{S1}]$$

Due to a double-pass (reflection imaging) geometry, the system PSF, $h(x, y, z; k) = \mu_r k^2 |P(k)|^2 g^2(x, y, z; k)$, is a product of the complex incident and (identical) collection beam, $g(x, y, z; k)$, where $|P(k)|^2$ is the optical power spectral density and μ_r determines the interferometric splitting ratio. The convolution theorem can be invoked to rewrite Eq. S1 in the transverse spatial frequency domain as

$$\tilde{S}(Q_x, Q_y; k) = \int H(Q_x, Q_y, z'; k) \tilde{\eta}(Q_x, Q_y, z') dz', \quad [\text{S2}]$$

where the tilde ($\tilde{}$) denotes the 2D transverse Fourier transform, and $H(Q_x, Q_y, z; k)$ encodes the (depth-dependent) transverse bandpass response of the effective PSF. The axial coordinate origin $z = 0$ is set at the nominal (aberration-free) beam focus. For the ideal case (with aberration-free beams), Eq. S2 can be simplified using asymptotic approximations for the near and far-from-focus regimes (2), to give the ISAM forward model (1, 2)

$$\tilde{S}(Q_x, Q_y; k) = H(Q_x, Q_y, k) \tilde{\tilde{\eta}}(Q_x, Q_y, Q_z), \quad [\text{S3}]$$

where the double tilde ($\tilde{\tilde{}}$) denotes the 3D Fourier transform, the filter $H(Q_x, Q_y, k)$ encodes the space-invariant axial and transverse spatial frequency response of the (ideal) system, and Q_z can be written as a function of k according to $Q_z = -\sqrt{4k^2 - Q_x^2 - Q_y^2}$. The interferometric synthetic aperture microscopy algorithm resamples $\tilde{S}(Q_x, Q_y; k)$ according to $k = \frac{1}{2} \sqrt{Q_x^2 + Q_y^2 + Q_z^2}$, in order to compute a bandpass filtered version of the 3D Fourier transform of the scattering potential.

Computational adaptive optics (AO) is based on computational corrections of the effects of pupil plane aberrations in the tomogram. The objective lens pupil function $P(x, y)$ is related to the focal-plane transverse frequency response of the single-pass illumination beam via the coordinate change $(x, y) = (-2\pi z_f Q_x/k, -2\pi z_f Q_y/k)$ (3), resulting in

$$\tilde{g}(Q_x, Q_y, 0; k) = P\left(\frac{-2\pi z_f Q_x}{k}, \frac{-2\pi z_f Q_y}{k}\right), \quad [\text{S4}]$$

where z_f is the (object-side) focal length of the objective lens. The beam aberration, Φ_g , is included in the generalized pupil function (3) $P(x, y) = P_{\text{ideal}}(x, y) e^{ik\Phi_g(x, y)}$, where $P_{\text{ideal}}(x, y)$ is a real Gaussian envelope. Because the ideal beam focus is the impulse response of the (single-pass) imaging system, $\tilde{g}(Q_x, Q_y, 0; k)$ can be regarded as the (transverse) amplitude transfer function (3).

Although hardware-based AO corrects beam aberrations, our goal is to correct the effects of aberrations in the system PSF, $h(x, y, z; k)$. We use Eq. S4 to relate pupil aberrations of the illumination beam to aberration artifacts in the system PSF. According to Eq. S4, pupil aberrations can be corrected in the (focal-plane) transverse frequency domain of the illumination beam. For an ideal focus, all transverse spatial frequencies interfere constructively, resulting in a uniform phase response for both the single-pass illumination beam and corresponding system PSF. Defining Φ_h as the deviation of the system focal-plane PSF from uniform transverse-frequency phase, and neglecting constant phase offsets, we obtain

$$\Phi_h\left(\frac{-2\pi z_f Q_x}{k}, \frac{-2\pi z_f Q_y}{k}\right) = \arg\left\{P\left(\frac{-2\pi z_f Q_x}{k}, \frac{-2\pi z_f Q_y}{k}\right) * P\left(\frac{-2\pi z_f Q_x}{k}, \frac{-2\pi z_f Q_y}{k}\right)\right\}, \quad [\text{S5}]$$

where the convolution, indicated by $*$, is performed over coordinates (Q_x, Q_y) . It is convenient to invoke the convolution theorem, and numerically evaluate the right-hand side of Eq. S5 as a product in the spatial domain.

Generally, aberrations in the pupil result in artifacts that vary with depth, and therefore require correction at each plane of reconstruction. Correcting these so-called space-variant aberration effects requires expensive (slow) computations. However, in some cases of interest, the dominant artifacts are space-invariant, and a more efficient approach may be taken. Space-invariant contributions of aberrations can be incorporated as a linear filter, $H_A(Q_x, Q_y; k)$, and we can rewrite the model in Eq. S3 as

$$\tilde{S}_A(Q_x, Q_y; k) \approx H_A(Q_x, Q_y; k) H(Q_x, Q_y, k) \tilde{\tilde{\eta}}(Q_x, Q_y, Q_z), \quad [\text{S6}]$$

where we only consider the phase contribution from the convolution in Eq. S5, to obtain the filter $H_A(Q_x, Q_y; k) = e^{ik\Phi_h(-2\pi z_f Q_x/k, -2\pi z_f Q_y/k)}$. The effect of this phase filter is simply inverted (by phase conjugation) to obtain an aberration correction filter, $H_{AC}(Q_x, Q_y; k) = e^{-ik\Phi_h(-2\pi z_f Q_x/k, -2\pi z_f Q_y/k)}$, and the signal with ideal (diffraction-limited) resolution restored to the focal plane is given by

$$\tilde{S}_{AC}(Q_x, Q_y; k) = H_{AC}(Q_x, Q_y; k) \tilde{S}_A(Q_x, Q_y; k). \quad [\text{S7}]$$

Space-variant effects of aberrations can be corrected via a 2D version of the aberration correction filter, and applied to $\tilde{S}(Q_x, Q_y, z_{\text{const}})$, at a given depth z_{const} (see Fig. 6 and Movie S1).

As in the case of hardware-based AO, we express the pupil phase aberrations of the beam, Φ_g , as a sum of Zernike polynomials, corresponding to specific, well-known, aberrations (4, 5). Although in principle it may be possible to compute Φ_g from a measurement of Φ_h , practically it is convenient to optimize the aberration correction filter based on the tomogram of a sample consisting of subresolution scatterers, or on visual inspection or image metrics applied to the sample of interest. For the results reported here, the aberration correction filter was optimized through image metrics (see *Methods*, Movie S1, and Fig. S1) applied to the *en face* planes at depths shown in Fig. 2, while tuning a 2D filter $[H_{AC,2D}(Q_x, Q_y) = e^{-ik_c \Phi_h(-2\pi z_f Q_x/k_c, -2\pi z_f Q_y/k_c)}$,

where k_c is the central wavenumber] that is applied to these planes (Movie S1 and Fig. S1). The 3D aberration correction fil-

ter was computed from this 2D filter as $H_{AC}(Q_x, Q_y; k) = e^{-i(k/k_c) \arg\{H_{AC,2D}(Q_x, Q_y)\}}$.

1. Ralston TS, Marks DL, Carney PS, Boppart SA (2006) Inverse scattering for optical coherence tomography. *J Opt Soc Am A* 23:1027–1037.
2. Davis BJ, et al. (2007) Nonparaxial vector-field modeling of optical coherence tomography and interferometric synthetic aperture microscopy. *J Opt Soc Am A* 24:2527–2542.
3. Goodman JW (1996) Introduction to Fourier Optics (McGraw-Hill, San Francisco), 2nd Ed., pp 135–137, 145–146.
4. Colomb T, et al. (2006) Numerical parametric lens for shifting, magnification, and complete aberration compensation in digital holographic microscopy. *J Opt Soc Am A* 23:3177–3190.
5. Malacara D (2007) *Optical Shop Testing* (Wiley-Interscience, Hoboken, NJ), 3rd Ed, p 519.

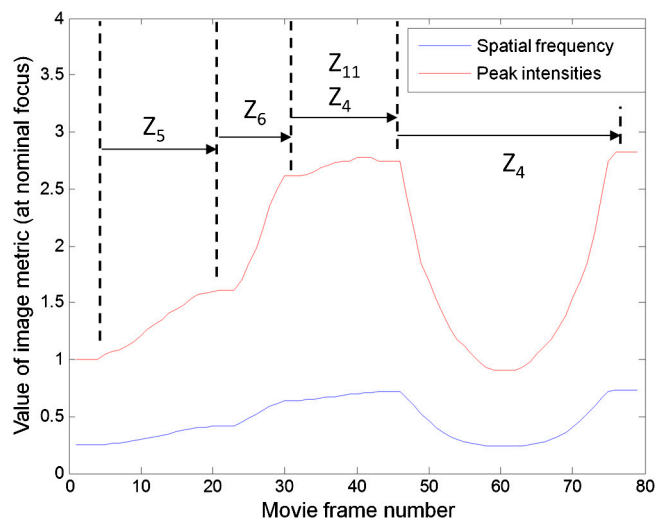


Fig. S1. Plot of the image metrics used to optimize the aberration correction, as a function of the movie frame number in Movie S1. The image metrics were calculated for the *en face* amplitude image corresponding to the plane of least confusion (which is also the nominal aberration-free focal plane). See *Methods* for details of the image metrics.

